## REFERENCES AND NOTES

1. M. Guatteri, P. Spudich, *Bull. Seismol. Soc. Am.* **90**, 98–116 (2000).
2. X. Lu, N. Lapusta, A. J. Rosakis, *Proc. Natl. Acad. Sci. U.S.A.* **104**, 18931–18936 (2007).
3. R. M. Nikolaidis *et al.*, *J. Geophys. Res. Solid Earth* **106**, 21897–21916 (2001).
4. G. L. Emore, J. S. Haase, K. Choi, K. A. Larson, A. Yamagiwa, *Bull. Seismol. Soc. Am.* **97**, 357–378 (2007).
5. J.-P. Avouac, L. Meng, S. Wei, W. Wang, J.-P. Ampuero, *Nat. Geosci.* (2015).
6. USGS, *M7.8 - 36km E of Khudi, Nepal* (2015); http://earthquake.usgs.gov/earthquakes/eventpage/us20002926.
7. T. Ader *et al.*, *J. Geophys. Res. Solid Earth* **117**, B04403 (2012).
8. NSET, *Gorkha Earthquake: Intensity Maps* (2015); www.nset.org.np/eq2015/intensity_maps.php.
9. J. L. Mugnier, P. Huyghe, A. P. Gajurel, B. N. Upreti, F. Jouanne, *Tectonophysics* **509**, 33–49 (2011).
10. R. Bilham, *Curr. Sci.* **69**, 101–128 (1995).
11. M. R. Pant, *Ādarśa* **2**, 29–60 (2002).
12. Kathamandu Valley Earthquake Risk Management Project, *The Kathmandu Valley Earthquake Risk Management Action Plan* (NSET, Lalitpur, Nepal, 1998); www.preventionweb.net/english/professional/publications/v.php?id=1496.
13. Y. R. Paudyal, R. Yatabe, N. P. Bhandary, R. K. Dahal, *Earthq. Eng. Eng. Vib.* **11**, 257–268 (2012).
14. S. Moribayashi, Y. Maruo, *J. Jap. Soc. Eng. Geol.* **21**, 80–87 (1980).
15. B. S. J. B. Rana, *Nepal Ko Maha Bhukampa (1990 Sala) Nepal's Great Earthquake* (Sahyogi Prakashan, Kathmandu, 1935).
16. The Nepal Geodetic Array (www.tectonics.caltech.edu/resources/kmlnepal.html) was deployed through a collaboration between the Caltech Tectonics Observatory (USA), the Department of Mines and Geology (Nepal), and the Department Analyse et Surveillance de l'Environnement (CEA, France).
17. USGS, *NetQuakes: Station KATNP_NQ_01*, 25 April 2015; http://earthquake.usgs.gov/monitoring/netquakes/station/KATNP_NQ_01/20150425061138/.
18. E. Lindsey *et al.*, *Nepal Earthquake: Line of Sight Deformation from ALOS-2 Interferometry*, 7 May 2015; http://topex.ucsd.edu/nepal.
19. European Space Agency, *Nepal Earthquake: Sentinel-1 InSAR Analysis*, April 2015; http://insarap.org/.
20. C. Ji, K. M. Larson, Y. Tan, K. W. Hudnut, K. H. Choi, *Geophys. Res. Lett.* **31**, L17608 (2004).
21. H. Yue *et al.*, *J. Geophys. Res. Solid Earth* **118**, 5453–5466 (2013).
22. T. H. Heaton, *Phys. Earth Planet. Inter.* **64**, 1–20 (1990).
23. D. Melgar, Y. Bock, *J. Geophys. Res. Solid Earth* **120**, 3324–3349 (2015).
24. Materials and methods are available as supplementary materials on *Science* Online.
25. R. S. Stein, *Nature* **402**, 605–609 (1999).
26. R. Bilham, K. Larson, J. Freymueller, *Nature* **386**, 61–64 (1997).
27. R. Cattin, J.-P. Avouac, *J. Geophys. Res. Solid Earth* **105**, 13389–13407 (2000).
28. E. Tinti, E. Fukuyama, A. Piatanesi, M. Cocco, *Bull. Seismol. Soc. Am.* **95**, 1211–1223 (2005).
29. S. Ide, M. Takeo, *J. Geophys. Res. Solid Earth* **102**, 27379–27391 (1997).
30. T. Mikumo, K. B. Olsen, E. Fukuyama, Y. Yagi, *Bull. Seismol. Soc. Am.* **93**, 264–282 (2003).
31. A. Bizzarri, M. Cocco, *J. Geophys. Res. Solid Earth* **108**, 2373 (2003).
32. J. E. Kozdon, E. M. Dunham, *Bull. Seismol. Soc. Am.* **103**, 1275–1289 (2013).
33. D. D. Oglesby, R. J. Archuleta, S. B. Nielsen, *Science* **280**, 1055–1059 (1998).
34. C. B. Worden, M. C. Gerstenberger, D. A. Rhoades, D. J. Wald, *Bull. Seismol. Soc. Am.* **102**, 204–221 (2012).



## ACKNOWLEDGMENTS

The GPS data are available from the UNAVCO website. The InSAR data are available at http://topex.ucsd.edu/nepal/. The Nepal Geodetic Array was funded by Caltech and DASE (to J.-P.A.) and by the Gordon and Betty Moore Foundation, through grant GBMF 423.01 to the Caltech Tectonics Observatory; support was maintained by NSF grant EAR-1345136. A. Miner and the Pacific Northwest Geodetic Array (PANGA) at CWU are thanked for technical assistance with the construction and operation of the Tribhuvan University (TU)–CWU network. Additional funding for the TU-CWU network came from the United Nations Development Programme and the Nepal Academy for Science and Technology. The high-rate data were recovered thanks to (i) a rapid intervention funded by NASA (USA) and the Department of Foreign International Development (UK) and (ii) engineering services provided by UNAVCO via the GAGE (Geodesy Advancing Geosciences and EarthScope) Facility, with support from NSF and NASA under NSF Cooperative Agreement no. EAR-1261833. We also thank Trimble Navigation and the Vaidya family for supporting the rapid response. The accelerometer record at KATNP was provided by USGS. We thank A. Nathan (U.S. Embassy in Kathmandu), S. Hough, D. Given, I. Flores, and J. Luetgert for contributions to the installation of this station. Research at UC–Berkeley was funded by the Gordon and Betty Moore Foundation through grant GBMF 3024. A portion of this work was carried out at JPL under a contract with the NASA. The GPS data were processed by the Advanced Rapid Imaging and Analysis Center for Natural Hazards (JPL) and the Scripps Orbit and Permanent Array Center. The effort at the Scripps Institution of Oceanography was funded by NASA grants NNX14AQ53G and NNX14AT33G. Advanced Land Observing Satellite–2 data were provided by the Japan Aerospace Exploration Agency under investigations 1148 and 1413. J.-P.A. thanks the Royal Society for support. We thank D. Dreger for discussion and W. Mooney for comments. J.-P.A led the study and wrote the article. D.M. performed the kinematic modeling and wrote the article. Y.B. supervised the high-rate data processing and wrote the article. J.Ga. led the field operations. J.Ge. conducted the high-rate data processing. S.O., A.M., W.S., and J.F.G. conducted the low-rate data analysis to estimate coseismic offsets. E.O.L. and X.X. conducted the InSAR data processing. L.B. helped to organize the field operations. All other authors contributed to building and servicing the GPS stations and to the post-earthquake data recovery. All authors edited the article.


## SUPPLEMENTARY MATERIALS

www.sciencemag.org/content/349/6252/1091/suppl/DC1
Materials and Methods
Figs. S1 to S11
Tables S1 and S2
Movie S1
References (*35*–*45*)

25 May 2015; accepted 29 July 2015
Published online 6 August 2015
10.1126/science.aac6383

SYNTHETIC BIOLOGY

# Complete biosynthesis of opioids in yeast

**Stephanie Galanie,[1] Kate Thodey,[2] Isis J. Trenchard,[2] Maria Filsinger Interrante,[2] Christina D. Smolke[2]***

**Opioids are the primary drugs used in Western medicine for pain management and palliative care. Farming of opium poppies remains the sole source of these essential medicines, despite diverse market demands and uncertainty in crop yields due to weather, climate change, and pests. We engineered yeast to produce the selected opioid compounds thebaine and hydrocodone starting from sugar. All work was conducted in a laboratory that is permitted and secured for work with controlled substances. We combined enzyme discovery, enzyme engineering, and pathway and strain optimization to realize full opiate biosynthesis in yeast. The resulting opioid biosynthesis strains required the expression of 21 (thebaine) and 23 (hydrocodone) enzyme activities from plants, mammals, bacteria, and yeast itself. This is a proof of principle, and major hurdles remain before optimization and scale-up could be achieved. Open discussions of options for governing this technology are also needed in order to responsibly realize alternative supplies for these medically relevant compounds.**

Opioids are an important class of medicines that include the analgesic morphine and the antitussive codeine. The World Health Organization (WHO) classifies these compounds as essential medicines because of their utility in treating severe pain, in pain management, and in palliative care (*1*). In the developing world, there are shortages of painkillers; the WHO has estimated that 5.5 billion people have "low to nonexistent access to treatment for moderate or severe pain" (*2*).

All natural opiates (e.g., morphine and codeine) and semisynthetic opioids (e.g., oxycodone, hydrocodone, and hydromorphone) are currently derived from the opium poppy (*Papaver somniferum*). Approximately 100,000 ha of opium poppy are cultivated annually to yield poppy straw containing more than 800 tons of opiates, primarily morphine and thebaine, to meet licit medical and scientific demand (*3*). The majority of poppy-derived morphine and thebaine is chemically converted into higher-value compounds, including codeine, oxycodone, and hydrocodone. Industrial poppy farming is susceptible to environmental factors such as pests, disease, and climate, which can introduce instability and variability into this geographically concentrated supply chain, resulting in pressure to diversify supply (*4*). Despite diverse market demands and increasing supply risks, poppy farming remains the sole source of opioids, in part because chemical synthesis of these complex molecules is not commercially competitive. Approximately 30 chemical syntheses

[1]Department of Chemistry, Stanford University, Stanford, CA 94305, USA. [2]Department of Bioengineering, Stanford University, Stanford, CA 94305, USA.
***Corresponding author. E-mail: csmolke@stanford.edu**

of morphine and derivatives have been reported (*5*), but none are feasible for large-scale production.

A microbial-based manufacturing process for opioids or opioid precursors, which are part of the larger class of benzylisoquinoline alkaloids (BIAs), has the potential to address many of the challenges associated with the poppy-based supply chain. Industrial cultivation of microorganisms, such as the baker's yeast *Saccharomyces cerevisiae*, occurs over days, whereas poppies are annuals. Also, because microbes are grown in closed fermentation vessels, the production process is not susceptible to external environmental factors and could provide greater consistency in product composition and impurity profiles across batches.

In recent years, researchers have engineered yeast to produce a variety of plant-based natural products (*6*), most notably artemisinic acid, a precursor to the antimalarial drug artemisinin (*7*). Semisynthetic production of artemisinin has now reached the market, meeting up to one-third of global need (*8*, *9*). Yeast-based production of artemisinic acid required the introduction of three to six heterologous plant genes and numerous genetic modifications to increase productivity (*7*, *9*). Although advances in synthetic biology have increased the complexity of plant pathways that can be reconstructed (*6*), all efforts to engineer yeast to produce BIAs downstream of (*S*)-reticuline, including morphinans, have relied on an external supply of BIA precursors (*10*–*15*). *Escherichia coli* (*16*) and, very recently, yeast (*17*, *18*) have been engineered to produce early BIA intermediates de novo; these accomplishments suggest that yeast might be capable of synthesizing opioids from simple carbon and nitrogen sources. We and others engineered the first part of the biosynthetic pathway, from tyrosine to (*S*)-reticuline (*17*, *18*). Separately, we engineered a second part of the pathway, from thebaine to morphine (*13*); others later engineered

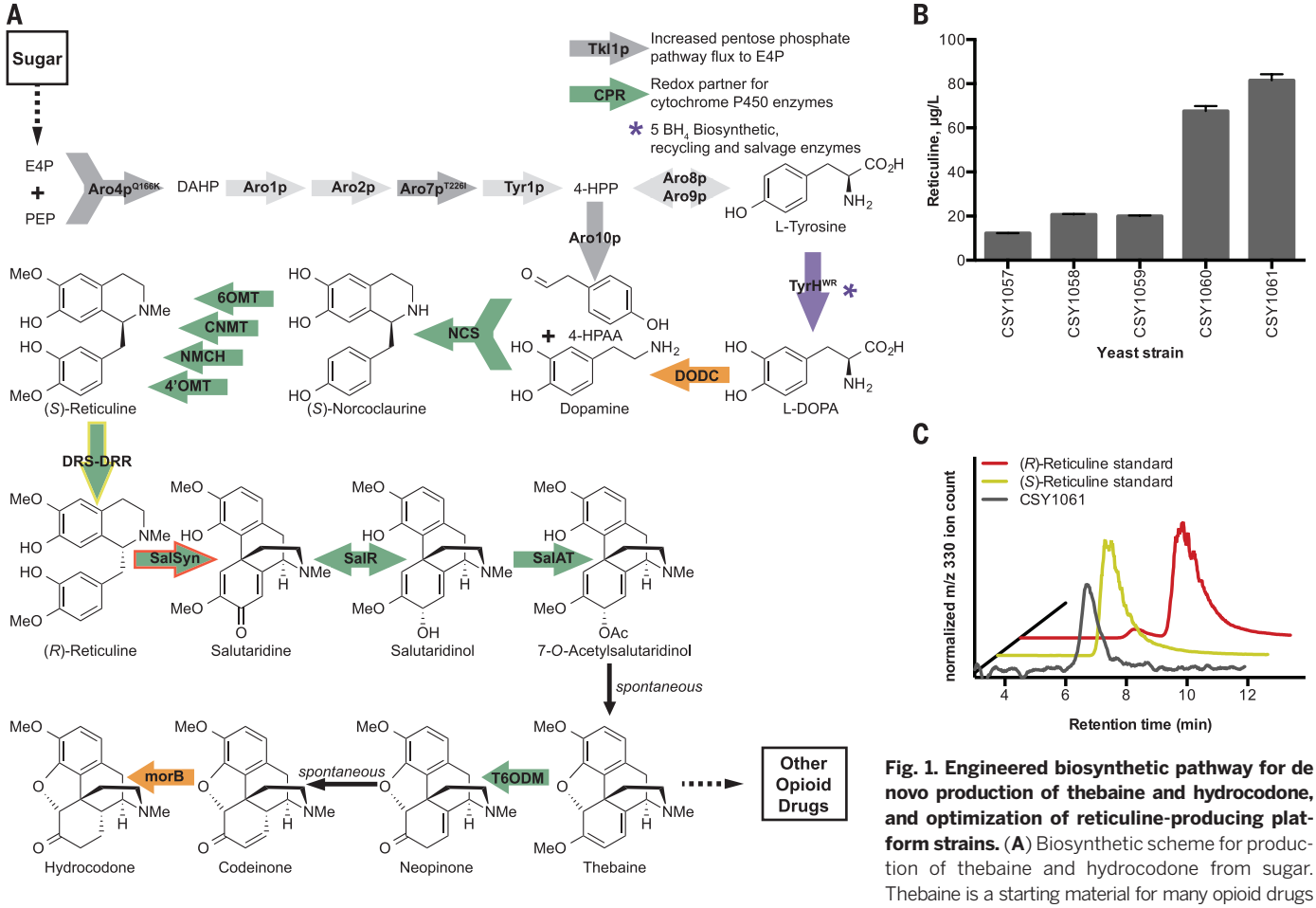


**Fig. 1. Engineered biosynthetic pathway for de novo production of thebaine and hydrocodone, and optimization of reticuline-producing platform strains.** (**A**) Biosynthetic scheme for production of thebaine and hydrocodone from sugar. Thebaine is a starting material for many opioid drugs through biosynthetic and semisynthetic routes. Block arrows indicate enzyme-catalyzed steps. Light gray arrows, unmodified yeast enzymes; dark gray arrows, overexpressed and modified yeast enzymes; purple arrows, mammalian (*Rattus norvegicus*) enzymes; orange arrows, bacterial (*Pseudomonas putida*) enzymes; green arrows, plant (*Papaver somniferum*, *P. bracteatum*, *Coptis japonica*, *Eschscholzia californica*) enzymes. Yellow outline highlights DRS-DRR; red outline highlights engineered SalSyn. E4P, erythrose 4-phosphate; PEP, phosphoenolpyruvate; DAHP, 3-deoxy-D-*arabino*-2-heptulosonic acid 7-phosphate; 4-HPP, 4-hydroxyphenylpyruvate; 4-HPAA, 4-hydroxyphenylacetaldehyde; $BH_4$, 5,6,7,8-tetrahydrobiopterin; Tkl1p, transketolase; CPR, cytochrome P450 reductase; Aro4p$^{Q166K}$, DAHP synthase; Aro1p, pentafunctional *arom* enzyme; Aro2p, bifunctional chorismate synthase and flavin reductase; Aro7p$^{T226I}$, chorismate mutase; Tyr1p, prephenate dehydrogenase; Aro8p, aromatic aminotransferase I; Aro9p, aromatic aminotransferase II; Aro10p, phenylpyruvate decarboxylase; TyrH$^{WR}$, feedback inhibition–resistant tyrosine hydroxylase (mutations R37E, R38E, W166Y); DODC, L-DOPA decarboxylase; NCS, (*S*)-norcoclaurine synthase; 6OMT, norcoclaurine 6-*O*-methyltransferase; CNMT, coclaurine *N*-methyltransferase; NMCH, *N*-methylcoclaurine hydroxylase; 4′OMT, 3′-hydroxy-*N*-methylcoclaurine 4′-*O*-methyltransferase; DRS-DRR, 1,2-dehydroreticuline synthase-1,2-dehydroreticuline reductase; SalSyn, salutaridine synthase; SalR, salutaridine reductase; SalAT, salutaridinol 7-*O*-acetyltransferase; T6ODM, thebaine 6-*O*-demethylase; morB, morphinone reductase. See figs. S1 and S2 for details of the $BH_4$ biosynthesis, recycling, and salvage pathway, conversion of (*S*)-norcoclaurine to (*S*)-reticuline, and genetic pathway modules. (**B**) Optimization of the reticuline-producing platform strain through pathway and strain engineering. Reticuline in the growth media was analyzed by LC-MS/MS multiple reaction monitoring (MRM) and quantified with an external standard curve. Error bars represent SD of three biological replicates. (**C**) Chiral analysis of reticuline produced by the platform strain. Reticuline was isolated from the growth medium of strain CSY1061 and separated on a chiral column. This chromatogram is one of two similar traces from replicate yeast cultures and was smoothed using a 7-point boxcar moving average.

a pathway from (*R*)-reticuline to codeine (*15*). However, functionally expressing the more than 20 heterologous genes required for complete biosynthesis of these complex molecules has been challenging because of the decreases in titer observed with each additional enzymatic step. Also, the key enzyme that epimerizes the (*S*)-benzylisoquinoline scaffold to the (*R*)-enantiomer, which is the biosynthetic precursor of the promorphinan and morphinan scaffolds, has remained unknown even after decades of study until recently identified by two groups (*19*, *20*) and by our team, as described below.

A decade ago, when we began work to realize total biosynthesis of opioids in yeast, we were motivated by the many foreseeable benefits yet mindful of potential negative impacts. Specifically, we were and remain concerned that a yeast-based opioid supply might contribute to opioid abuse (*21*, *22*). Thus, before starting this project, we sought and received permission to carry it out via Stanford University's institutional research registration with the U.S. Drug Enforcement Agency (DEA). Gaining permission required (i) background screening for researchers handling Schedule II compounds or yeast strains capable of making such compounds; (ii) detailed protocols limiting fermentation volumes and compound concentrations and including provisions for culture and product destruction and disposal immediately after experiments; (iii) increased physical containment for the strains and controlled compounds; (iv) increased laboratory security; and (v) explicit management and reporting. Taken together, these requirements reduce the chance that any compounds or strains generated in our research would directly enable individuals to abuse opioids.

We first built a yeast strain to produce (*S*)-reticuline, a key biosynthetic intermediate to many downstream BIAs including the morphinans. This strain was built with a new modular genetic design that incorporated modifications designed to divert greater carbon flux through tyrosine to (*S*)-reticuline. The reticuline biosynthetic pathway was split into four genetic modules that contain the coding sequences for 17 biosynthetic enzymes (Fig. 1A, figs. S1 and S2, and table S1). We selected chromosomal regions from which we expected no growth defect and active expression as integration loci (*23*–*25*). A precursor overproduction module (I) designed to increase accumulation of L-tyrosine and 4-hydroxyphenylacetaldehyde (4-HPAA) encoded the overexpression of three or four yeast proteins—mutants of 3-deoxy-D-*arabino*-2-heptulosonic acid 7-phosphate (DAHP) synthase and chorismate mutase ($Aro4p^{Q166K}$, $Aro7p^{T226I}$) that are less inhibited by L-tyrosine, and transketolase (Tkl1p); additionally, phenylpyruvate decarboxylase (Aro10p) was included in a second version of this module (fig. S2). A tetrahydrobiopterin ($BH_4$) module (II) designed to synthesize and recycle this mammalian redox cofactor encoded the expression of four proteins from *Rattus norvegicus*: sepiapterin reductase (SepR), 6-pyruvoyl tetrahydrobiopterin synthase (PTPS), quinonoid dihydropteridine reductase (QDHPR), and pterin carbinolamine dehydratase (PCD). An (*S*)-norcoclaurine module (III) designed to synthesize the first BIA backbone molecule encoded the expression of four proteins: a mutant of tyrosine hydroxylase ($TyrH^{WR}$; mutations R37E, R38E, W166Y) that is less inhibited by L-tyrosine and catecholamines, from *R. norvegicus*; the $BH_4$ salvage enzyme dihydrofolate reductase (DHFR), also from *R. norvegicus*; DOPA decarboxylase (DoDC) from the bacteria *Pseudomonas putida*; and norcoclaurine synthase (NCS) from the plant *Coptis japonica*. An (*S*)-reticuline module (IV) designed to synthesize the key BIA branchpoint molecule encoded the expression of five plant proteins, four from *P. somniferum*—norcoclaurine 6-*O*-methyltransferase (6OMT), coclaurine-*N*-methyltransferase (CNMT), 4′-*O*-methyltransferase (4′OMT), and cytochrome P450 reductase (CPR)—as well as *N*-methylcoclaurine hydroxylase (NMCH) from *Eschscholzia californica*. The enzyme variants were selected on the basis of examined activities in engineered yeast (*11*, *18*) and incorporated the addition of several new activities (i.e., Aro10p, DHFR) to increase flux to reticuline biosynthesis.

The BIA modules were integrated into a wild-type haploid CEN.PK2 strain. We assayed reticuline production by growing yeast strains in minimal synthetic complete media supplemented with ascorbic acid without ammonium sulfate for 72 hours (fig. S3) and analyzing the growth media for BIA molecules by liquid chromatography coupled with tandem mass spectrometry (LC-MS/MS) (table S2). A minimal reticuline-producing strain (CSY1057; table S3), which incorporated modules II to IV, produced reticuline with a titer of 12.3 μg/liter (Fig. 1B, fig. S4A, and table S4). The addition of module I to the strain, increasing BIA precursor supply, resulted in a factor of 1.6 improvement in reticuline accumulation, with or without Aro10p (CSY1059, 20.0 μg/liter; CSY1058, 20.7 μg/liter). We observed nearly complete consumption of L-DOPA (90 μg/liter; fig. S4B and table S4), substantial accumulation of dopamine (10 mg/liter; fig. S4C), and accumulation of 3′-hydroxy-*N*-methylcoclaurine (fig. S4, D and E) by LC-MS/MS for the strain harboring modules I to IV (CSY1059). We hypothesized that (i) increased expression of NCS

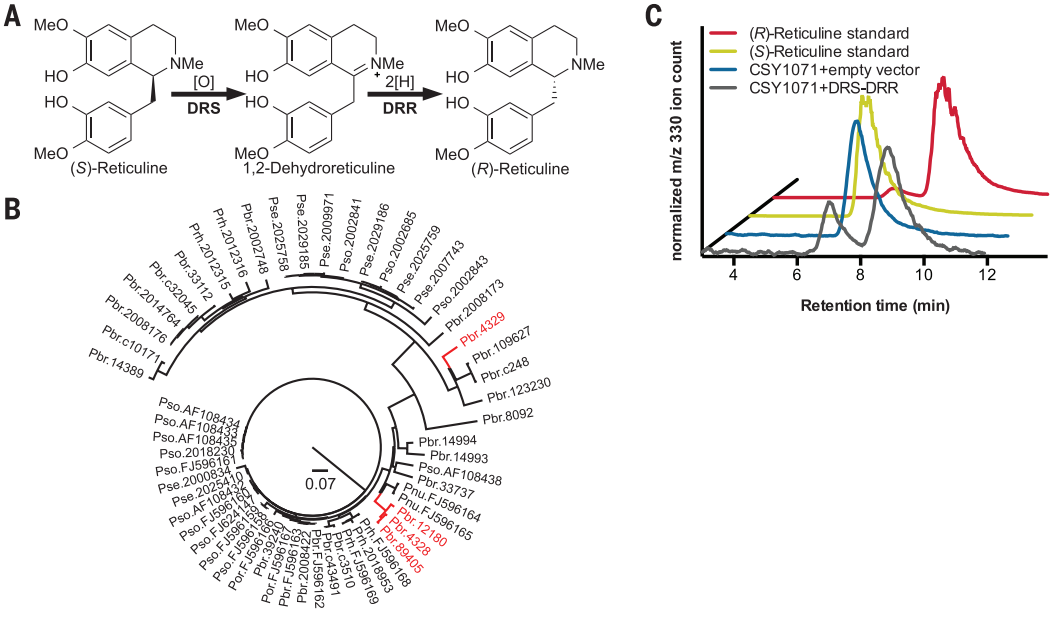


**Fig. 2. DRS-DRR converts (*S*)-reticuline to (*R*)-reticuline.** (**A**) Biosynthetic scheme for the reaction catalyzed by DRS-DRR; Me, methyl. (**B**) Identification of DRS-DRR via bioinformatic analysis of COR-like sequences. Bioinformatic query was COR VIGS sequence. Subject sequences were the *P. bracteatum* PhytoMetaSyn transcriptome; *P. bracteatum*, *P. setigerum*, *P. somniferum*, and *P. rhoeas* transcriptomes from the 1000 Plants Project; and all deposited sequences in GenBank belonging to *Papaveraceae*. The scale bar indicates amount of genetic change in amino acid substitutions per site. Branches highlighted in red indicate sequences containing both CYP and COR-like domains. Phylogenetic tree was generated using ClustalX bootstrap neighbor-joining tree with 1000 trials. (**C**) Chiral analysis of reticuline produced by yeast strains expressing and not expressing the enzyme DRS-DRR. Chiral analysis of reticuline accumulated in the growth media of strain CSY1071 with empty vector or DRS-DRR (pCS3301) was performed as described in Fig. 1C. This chromatogram is one of two similar traces from replicate yeast cultures and was smoothed using a 7-point boxcar moving average.

would increase conversion of dopamine and the native yeast metabolite 4-HPAA to norcoclaurine and downstream products, (ii) increased expression of TyrH$^{WR}$ would replenish the supply of dopamine, and (iii) increased expression of 4´OMT would reduce accumulation of 3´-hydroxy-*N*-methylcoclaurine and increase flux to reticuline. Thus, we designed a bottleneck module (V), which encoded the overexpression of three proteins—TyrH$^{WR}$, 4´OMT, and NCS—by incorporation of additional gene copies. The module was integrated into CSY1059 and designed to knock out the native *ZWF1* gene (*zwf1*Δ; CSY1061) or to integrate into a separate locus (CSY1060). A yeast platform strain with the addition of module V into the *zwf1* locus resulted in a further factor of 4 improvement in reticuline accumulation (82 μg/liter; Fig. 1B and table S4) and a corresponding factor of 2 decrease in accumulated 3´-hydroxy-*N*-methylcoclaurine relative to CSY1059 (fig. S4D).

Reticuline produced by the yeast platform strain CSY1061 was isolated by reverse-phase high-performance liquid chromatography and analyzed by chiral LC-MS. The chiral analysis indicated that the majority of the reticuline produced is the (*S*)-enantiomer (Fig. 1C), as was expected because of the stereospecificity of the NCS-catalyzed condensation. The production of primarily the (*S*)-enantiomer in our platform strain corroborates similar observations from other bacteria and yeast engineered with the three methyltransferase enzymes, even when fed racemic substrates (*10*, *15*–*17*). Opium poppy has the unique ability to convert (*S*)-reticuline to (*R*)-reticuline, from which the morphinan alkaloids are derived (*26*, *27*). Although extensive isotope feeding and biochemical studies have indicated that the epimerase activity proceeds via oxidation to a Schiff base intermediate and stereospecific reduction (Fig. 2A), the 1,2-dehydroreticuline synthase (DRS) and 1,2-dehydroreticuline reductase (DRR) enzyme(s) had not been isolated and sequenced when we began our study (*27*–*29*). While we were preparing this manuscript for submission, one group reported the discovery of this enzyme in *P. somniferum* by characterizing mutant alleles from chemically mutagenized opium poppy plants (*19*). While our manuscript was under review, another group reported using plant transcriptome databases to identify candidates and then cloned the gene from *P. somniferum* cDNA (*20*). Our approach instead leveraged plant transcriptome databases, DNA synthesis, and the engineered (*S*)-reticuline–producing yeast strains, thus not requiring access to physical plant material.

More specifically, we noted that two independent plant gene-silencing studies found that codeinone reductase (COR) knockdown results in reticuline accumulation, and in one case specifically (*S*)-reticuline accumulation (*30*, *31*). We hypothesized that a COR-like enzyme may catalyze the stereospecific reduction and used the published virus-induced gene silencing (VIGS) sequence as a BLAST query against *Papaver* species in the 1000 Plants Project (*32*) and PhytoMetaSyn (*33*, *34*) transcriptome databases. Hit identity was determined by a reverse BLAST search against sequences deposited in GenBank. Of the 38 COR-like sequences identified that were also greater than 300 nucleotides in length, four had a cytochrome P450 oxidase (CYP) 82Y1-like domain and a COR-like domain in a single open reading frame (DRS-DRR; Fig. 2B). We considered that this natural fusion protein could catalyze both the oxidation and reduction necessary for (*S*)-reticuline epimerization. We propose that the oxidation to 1,2-dehydroreticuline may occur via either a carbinolamine or enamine intermediate, and that 1,2-dehydroreticuline is then stereospecifically reduced to (*R*)-reticuline by the COR-like DRR domain (fig. S5).

To identify additional variants of this coding sequence and determine how widespread it is in nature, we used the amino acid sequence from *P. bracteatum* DRS-DRR (Pbr.89405) to search both databases by translated BLAST nucleotides (tBLASTn). A search of all sequences in the PhytoMetaSyn database (67 plant species) and the 1000 Plants Project transcriptome database (1328 assemblies derived from a few hundred plant species) identified a total of five apparent full-length and 10 partial unique sequences that harbored both domains (fig. S6), which originated from *P. somniferum* (opium poppy), *P. setigerum* (poppy of Troy), *P. bracteatum* (Iranian poppy), or *Chelidonium majus* (greater celandine). From this secondary search (fig. S6), we identified a *P. somniferum* DRS-DRR sequence of interest, Pso.2062398, which was a full-length sequence that had consensus with several individual transcriptome hits.

To determine whether the identified DRS-DRR enzyme possesses epimerase activity, we characterized the DRS-DRR enzyme in the context of a yeast strain engineered to produce (*S*)-reticuline from fed *rac*-norlaudanosoline (CSY1071; fig. S1C) (*11*). In preliminary experiments, we screened the three variants from *P. bracteatum* that clustered together in the initial search—Pbr.89405, Pbr.12180, and Pbr.4328—in strain CSY1071 with low-copy plasmids harboring expression cassettes for yeast codon–optimized DRS-DRR and yeast codon–optimized *P. somniferum* salutaridine synthase (yPsSalSyn). Codon optimization of all synthetic genes was performed by Life Technologies (*35*). When fed 1 mM norlaudanosoline, only the strain encoding DRS-DRR variant Pbr.89405 produced substantial salutaridine. We cultured strain CSY1071 containing the low-copy plasmid harboring this *DRS-DRR* (Pbr.89405, pCS3301) with 1 mM *rac*-norlaudanosoline for 72 hours, and isolated reticuline from the growth media for chiral LC-MS analysis. In strains expressing the DRS-DRR, more than half of the reticuline produced was the (*R*)-enantiomer, whereas exclusively (*S*)-reticuline was detected in strains lacking the DRS-DRR gene (Fig. 2C).

We next examined the activity of DRS-DRR enzyme variants in the context of the downstream conversion steps to thebaine, the first morphinan alkaloid in opiate biosynthesis. In preliminary experiments, yeast codon–optimized salutaridine reductase (SalR) variants from *P. bracteatum* and *P. somniferum* and site-directed mutants that were reported to reduce substrate inhibition and

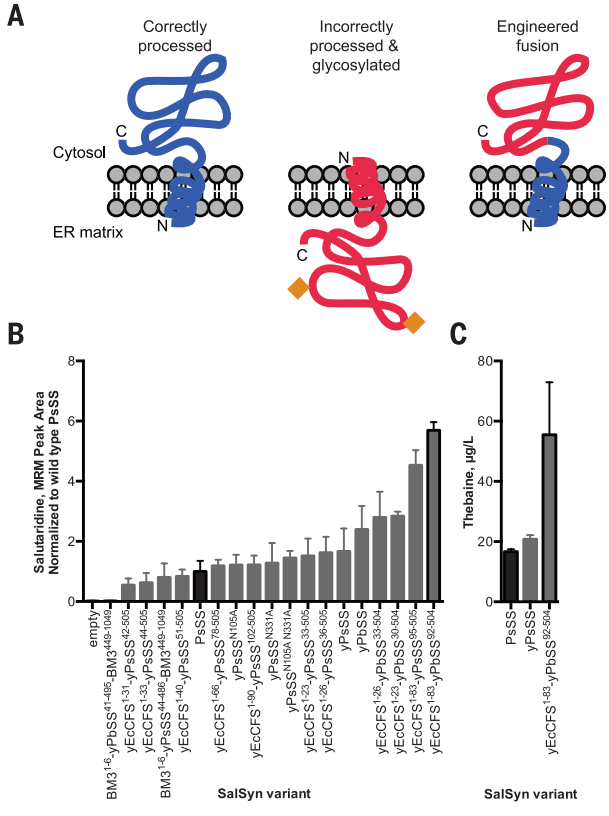


**Fig. 3. Engineered SalSyn chimeras improve conversion of (*R*)-reticuline to salutaridine.** (**A**) Schematic of the chimeric SalSyn engineering strategy to address incorrect processing and glycosylation of the wild-type SalSyn in yeast. Orange diamonds represent glycosylation. (**B**) Comparison of salutaridine produced from SalSyn variants, site-directed glycosylation mutants, and engineered fusions in yeast. Yeast strains expressing the indicated SalSyn variant were fed 10 μM (*R*)-reticuline, and the growth medium was analyzed by LC-MS/MS MRM. Peak areas were normalized to wild-type SalSyn (black). (**C**) Comparison of thebaine produced from SalSyn variants in yeast. Yeast strains were fed 1 mM *rac*-norlaudanosoline, and thebaine in the growth medium was quantified by LC-MS/MS MRM with an external standard curve. Bars outlined in black denote wild-type and best engineered variant. Error bars are SD of at least three biological replicates.

increase the maximum rate of reaction $V_{max}$ (*36*, *37*) were examined for their ability to catalyze conversion of salutaridine to thebaine with yeast codon–optimized salutaridinol acetyltransferase (SalAT) variants from *P. somniferum*, *P. bracteatum*, and *P. orientale*. The *P. bracteatum* SalR (PbSalR) and *P. somniferum* SalAT (PsSalAT) enzymes exhibited the highest activities in yeast (fig. S7, A and B). A yeast artificial chromosome (YAC, pCS3308) encoding expression cassettes for yPsSalSyn, PbSalR, and PsSalAT was assembled into strain CSY1071, and DRS-DRR variants were expressed from low-copy plasmids (pCS3300–3305). The resulting strains were assayed by feeding 1 mM *rac*-norlaudanosoline for 72 hours, and the growth medium was analyzed for thebaine production. *P. bracteatum* and *P. somniferum* DRS-DRR enzymes (Pbr.89405, Pso.2062398) resulted in similar thebaine production (fig. S7C), and the *P. bracteatum* DRS-DRR (PbDRS-DRR) was used in subsequent experiments. Expression cassettes for the four genes were assembled into a YAC (pCS3309) in strain CSY1071, and the resulting strain was assayed for thebaine production from fed *rac*-norlaudanosoline. This strain produced thebaine at a concentration of 17 μg/liter when cultured with 1 mM *rac*-norlaudanosoline for 96 hours (Fig. 3C and table S5). However, substantial accumulation of the intermediate reticuline (~660 μg/liter) was observed.

Because DRS-DRR is fairly efficient in the conversion of (*S*)- to (*R*)-reticuline (Fig. 2C), the accumulation of reticuline indicated that the conversion of (*R*)-reticuline to salutaridine, catalyzed by SalSyn, warranted further optimization. Western blot analysis indicated that yeast-expressed SalSyn protein was present as three forms that could be distinguished by apparent molecular weight, whereas SalSyn transiently expressed in *Nicotiana benthamiana* (tobacco) was present primarily at the lowest of these three apparent molecular weights (fig. S8A). Site-directed mutagenesis of three potential N-linked glycosylation sites [Asn-X-Thr/Ser (N-X-T/S)] indicated that the three bands arose from glycosylation of the protein at two sites, $Asn^{105}$ and $Asn^{331}$. N-linked glycosylation in yeast is indicative of incorrect N-terminal sorting of the nascent SalSyn polypeptide to the lumen of the endoplasmic reticulum (ER), where it is N-glycosylated rather than anchoring the N terminus in the outer ER membrane and maintaining the catalytic domain in the cytosol, as is typical of microsomal CYPs (Fig. 3A and fig. S8B) (*38*, *39*). We hypothesized that this misprocessing reduced SalSyn activity in yeast. However, modifying the glycosylation pattern of SalSyn by mutating the glycosylation sites reduced conversion of (*R*)-reticuline to salutaridine relative to the wild-type yeast codon–optimized enzyme (Fig. 3B).

We performed protein engineering to correct N-terminal sorting of the nascent SalSyn polypeptide, prevent N-linked glycosylation, and improve the enzyme's activity in yeast. Cheilanthifoline synthase (CFS) is a plant cytochrome P450 that is 61 to 68% identical to SalSyn, exhibits high activity when expressed in yeast (*14*), and is not glycosylated in yeast despite having one N-X-T/S site identical to the SalSyn sequence (fig. S8C). We designed yeast codon–optimized coding sequences for chimeric proteins with one or more N-terminal α helices from CFS replacing those of SalSyn variants from *P. somniferum* and *P. bracteatum*, with junction points for the fusions selected on the basis of amino acid alignments and/or protein secondary structure motifs. Western blot analysis of the chimeric proteins indicated that several of the engineered SalSyn enzymes were present as a single band in yeast, similar to the expression pattern observed for the plant-expressed parent enzyme (fig. S8D). The data indicated that the misprocessing of the nascent protein in yeast that resulted in N-linked glycosylation was repaired by the engineered fusions. As an alternative strategy, the coding sequence for the SalSyn CYP domain was cloned in place of the CYP domain in the cytosolic *Bacillus megaterium* P450 monooxygenase CYP102A1 (BM3), resulting in a chimeric protein with fused CYP and cytochrome P450 reductase domains. The chimeric SalSyn proteins were expressed from a low-copy plasmid in CSY1071 and assayed for salutaridine production from fed (*R*)-reticuline. Several of the engineered SalSyn variants exhibited improved activity relative to both the wild-type and codon-optimized enzymes, with the engineered *P. bracteatum* variant $yEcCFS^{1\text{-}83}$-$yPbSalSyn^{92\text{-}504}$ exhibiting greater conversion of (*R*)-reticuline to salutaridine by a factor of ~6 (Fig. 3B) and greater conversion of *rac*-norlaudanosoline to thebaine by a factor of >3 (55 μg/liter; Fig. 3C and table S5) relative to wild-type PsSalSyn.

To engineer a yeast strain that produces thebaine from simple carbon and nitrogen sources, we designed a thebaine module (VI) that encodes the expression of the best enzyme variants identified in our work—PbDRS-DRR, $yEcCFS^{1\text{-}83}$-$yPbSalSyn^{92\text{-}504}$, PbSalR, and PsSalAT—to convert (*S*)-reticuline to the morphinan alkaloid thebaine. Thebaine is extracted from opium poppy for use in semisynthesis of a number of opioids. This module was added to the reticuline-producing platform strain (CSY1060) as a chromosomal integration (CSY1064). The resulting strains were cultured in minimal media for 120 hours and the growth media assayed for thebaine (Fig. 4, A and B). These strains—containing 24 heterologous expression cassettes, 21 new enzyme activities, overexpression of two native enzymes, and inactivation of one native enzyme—produced thebaine at concentrations of 6.4 ± 0.3 μg/liter (table S6). We further extended the reconstructed biosynthetic pathway to a downstream opioid drug, hydrocodone (Fig. 1A), which is a main component in the second most dispensed prescription medicine in the United States (*40*). A hydrocodone module (VII), which encodes the expression of thebaine 6-*O*-demethylase (T6ODM) from *P. somniferum* and morphine reductase (morB) from *P. putida M10* (*13*), was introduced as a YAC (pCS2765) into the thebaine-producing strain CSY1064. The resulting strain was cultured in minimal media with 50 mM 2-oxoglutarate to support T6ODM activity for 120 hours and the growth media assayed for opioid compounds (Fig. 4, C and D, and table S6). The engineered yeast were able to produce low levels of hydrocodone, ~0.3 μg/liter. Thus, we have demonstrated the feasibility of extending the pathway to compounds of interest through a biosynthetic

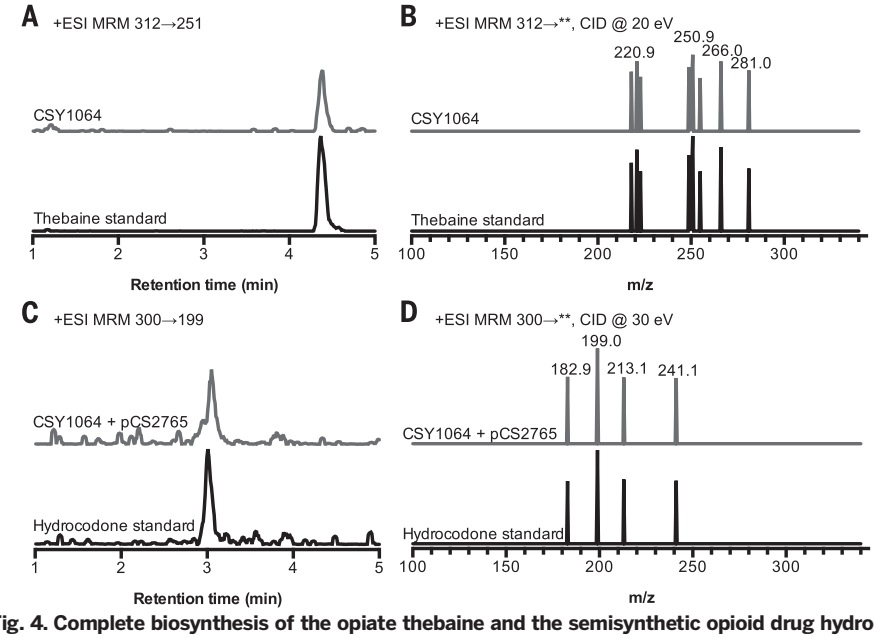


**Fig. 4. Complete biosynthesis of the opiate thebaine and the semisynthetic opioid drug hydrocodone in yeast.** (**A**) Chromatograms of thebaine detected in CSY1064 media and in a thebaine standard (7.8 μg/liter, 25 nM). (**B**) Spectra of eight MRM transitions of thebaine produced by engineered yeast and the thebaine standard. (**C**) Chromatograms of hydrocodone detected in CSY1064+pCS2765 media and in a hydrocodone standard (0.3 μg/liter, 1 nM). (**D**) Spectra of four MRM transitions of hydrocodone produced by engineered yeast and the hydrocodone standard. Growth medium was analyzed for opioids by LC-MS/MS MRM. Traces are representative of four biological replicates.

route that is not present in the native opium poppy without having to incorporate downstream chemical synthesis.

This work represents the complete biosynthesis of opiates in a heterologous host starting from central metabolism. Through our synthetic approach, we validated the capability of DRS-DDR variants from different plants to catalyze the (*S*)- to (*R*)-epimerization of reticuline in the context of the heterologous opiate biosynthetic pathway. The engineering of yeast able to convert central metabolites to the complex pentacyclic morphinan scaffold required enzyme engineering to correct the processing and increase the activity of the key pathway cytochrome P450 leading to the promorphinan scaffold (SalSyn), as well as pathway and strain optimization, including the expression of 21 heterologous enzymes from plants, mammals, bacteria, and yeast, overexpression of two native yeast enzymes, and deletion of one native yeast gene. The current report represents a proof of principle for generating morphinan scaffolds de novo in yeast, and opens the possibility of derivatizing these and other molecules by new biosynthetic or semisynthetic routes to improve their therapeutic properties.

Fermentation titers of ~5 g/liter would be required for yeast-based production of opioids to be a feasible alternative to poppy farming for commercial production. As this represents a yield increase of more than five orders of magnitude, the strains reported here would not be suitable for commercial scale-up. Future engineering efforts could take advantage of the pathway's role as an electron sink for fermentative production to direct greater electron and carbon flux to the opiates rather than to ethanol or other fermentation products. At commercial productivities, ~5 ml of yeast grown over several days would provide one dose of pain medication, which is currently sourced from 0.2 $m^2$ of poppy field land over the course of a year; sourcing opiates from sugar and yeast instead of opium poppy could decrease the overall land area required for production by a factor of >500.

There is some concern that biosynthesis of opioids in yeast may soon lead to "home brew" opiates (*41*). The production levels achieved here under controlled fermentation conditions do not enable home brew of these drugs and also are not economically competitive with poppy farming for supplying either licit or illicit markets. Specifically, at the titers reported here (<1 μg/liter), a single dose of hydrocodone, as used in Vicodin (5 mg), would require thousands of liters of fermentation broth, which no home brewer would reasonably pursue. Such improvements are not merely a matter of fermentation scale-up and would require additional research to achieve the necessary strain and pathway improvements. Thus, the work reported here does not provide a "recipe" for making opioid drugs in a manner that directly undermines public health or security. Nonetheless, as a safeguard of future public health, our yeast strains only produce opioids (e.g., hydrocodone, thebaine) with reduced potential for diversion to illicit markets due to the added steps and cost of chemically converting these specific compounds to heroin. Although such strains could potentially be further engineered to produce morphine directly, prior work to convert thebaine to morphine realized only a 1.5% yield (*13*). Thus, as a rough estimate, a strain that converts sugar to morphine would require an improvement in overall yield by a factor of ~$7 \times 10^6$ relative to the work reported here.

Despite this precaution, substantially improved production of opioids via yeast should be expected in the next several years. More broadly, our work highlights the potential of yeast as a chassis for bio-based production of many complex chemicals and materials. Synthetic biology is poised to replace or supplement many supply chains with advanced bio-based manufacturing. A greatly expanded capacity to build with biology will contribute to changes in land and natural resource use, employment, and policy. Practical strategies that address concerns while enabling innovation and the realization of benefits must be developed now in order to secure our future bioeconomy. Given the complexity and diversity of both the potential concerns and possible benefits, we would strongly endorse an open deliberative process that develops options for the governance (*42*) of medicinal compound biosynthesis before economically competitive processes are realized.

## REFERENCES AND NOTES


1. World Health Organization, "18th WHO essential medicines list" (Geneva, Switzerland, 2013).
2. M. J. Seya, S. F. Gelders, O. U. Achara, B. Milani, W. K. Scholten, *J. Pain Palliat. Care Pharmacother.* **25**, 6–18 (2011).
3. International Narcotics Control Board, "Narcotic drugs: Estimated world requirements for 2015—statistics for 2013" (2014).
4. K. Bradsher, "Shake-up on opium island." *New York Times* (20 July 2014); www.nytimes.com/2014/07/20/business/international/tasmania-big-supplier-to-drug-companies-faces-changes.html.
5. J. W. Reed, T. Hudlicky, *Acc. Chem. Res.* **48**, 674–687 (2015).
6. M. S. Siddiqui, K. Thodey, I. Trenchard, C. D. Smolke, *FEMS Yeast Res.* **12**, 144–170 (2012).
7. D. K. Ro *et al*., *Nature* **440**, 940–943 (2006).
8. PATH, "Stabilizing the antimalarial drug supply: Semisynthetic artemisinin could meet up to one-third of global need" (2014); www.path.org/publications/detail.php?i=2438.
9. C. J. Paddon, J. D. Keasling, *Nat. Rev. Microbiol.* **12**, 355–367 (2014).
10. H. Minami *et al*., *Proc. Natl. Acad. Sci. U.S.A.* **105**, 7393–7398 (2008).
11. K. M. Hawkins, C. D. Smolke, *Nat. Chem. Biol.* **4**, 564–573 (2008).
12. E. Fossati *et al*., *Nat. Commun.* **5**, 3283 (2014).
13. K. Thodey, S. Galanie, C. D. Smolke, *Nat. Chem. Biol.* **10**, 837–844 (2014).
14. I. J. Trenchard, C. D. Smolke, *Metab. Eng.* **30**, 96–104 (2015).
15. E. Fossati, L. Narcross, A. Ekins, J. P. Falgueyret, V. J. Martin, *PLOS ONE* **10**, e0124459 (2015).
16. A. Nakagawa *et al*., *Nat. Commun.* **2**, 326 (2011).
17. W. C. DeLoache *et al*., *Nat. Chem. Biol.* **11**, 465–471 (2015).
18. I. J. Trenchard, M. S. Siddiqui, K. Thodey, C. D. Smolke, *Metab. Eng.* **31**, 74–83 (2015).
19. T. Winzer *et al*., *Science* **349**, 309–312 (2015).
20. S. C. Farrow, J. M. Hagel, G. A. W. Beaudoin, D. C. Burns, P. J. Facchini, *Nat. Chem. Biol.* 10.1038/nchembio.1879 (2015).
21. T. Gomes *et al*., *Addiction* **109**, 1482–1488 (2014).
22. D. B. Reuben *et al*., *Ann. Intern. Med.* **162**, 295–300 (2015).
23. E. J. Dean, J. C. Davis, R. W. Davis, D. A. Petrov, *PLOS Genet.* **4**, e1000113 (2008).
24. I. Nogae, M. Johnston, *Gene* **96**, 161–169 (1990).
25. D. Bai Flagfeldt, V. Siewers, L. Huang, J. Nielsen, *Yeast* **26**, 545–551 (2009).
26. A. R. Battersby, D. M. Foulkes, R. Binks, *J. Chem. Soc.* **33**, 3323–3332 (1965).
27. K. Hirata, C. Poeaknapo, J. Schmidt, M. H. Zenk, *Phytochemistry* **65**, 1039–1046 (2004).
28. G. A. Beaudoin, P. J. Facchini, *Planta* **240**, 19–32 (2014).
29. W. DeEknamkul, M. H. Zenk, *Phytochemistry* **31**, 813–821 (1992).
30. R. S. Allen *et al*., *Nat. Biotechnol.* **22**, 1559–1566 (2004).
31. C. P. Wijekoon, P. J. Facchini, *Plant J.* **69**, 1052–1063 (2012).
32. N. Matasci *et al*., *Gigascience* **3**, 17 (2014).
33. P. J. Facchini *et al*., *Trends Biotechnol.* **30**, 127–131 (2012).
34. M. Xiao *et al*., *J. Biotechnol.* **166**, 122–134 (2013).
35. S. Fath *et al*., *PLOS ONE* **6**, e17596 (2011).
36. J. Ziegler, W. Brandt, R. Geissler, P. J. Facchini, *J. Biol. Chem.* **284**, 26758–26767 (2009).
37. Y. Higashi, T. M. Kutchan, T. J. Smith, *J. Biol. Chem.* **286**, 6532–6541 (2011).
38. V. Goder, M. Spiess, *FEBS Lett.* **504**, 87–93 (2001).
39. M. Higy, T. Junne, M. Spiess, *Biochemistry* **43**, 12716–12722 (2004).
40. IMS Institute for Healthcare Informatics, "Medicines use and spending shifts: A review of the use of medicines in the U.S. in 2014" (2015); www.imshealth.com/portal/site/imshealth/menuitem.762a961826aad98f53c753c71ad8c22a/?vgnextoid=3f140a4331e8c410VgnVCM1000000e2e2ca2RCRD.
41. K. A. Oye, J. C. Lawson, T. Bubela, *Nature* **521**, 281–283 (2015).
42. M. S. Garfinkel, D. Endy, G. L. Epstein, R. M. Friedman, *Biosecur. Bioterror.* **5**, 359–362 (2007).
43. S. Alberti, A. D. Gitler, S. Lindquist, *Yeast* **24**, 913–919 (2007).
44. R. D. Gietz, R. H. Schiestl, *Nat. Protoc.* **2**, 31–34 (2007).
45. D. G. Gibson *et al*., *Nat. Methods* **6**, 343–345 (2009).
46. G. Chao *et al*., *Nat. Protoc.* **1**, 755–768 (2006).
47. J. H. Hegemann, U. Güldener, G. J. Köhler, *Methods Mol. Biol.* **313**, 129–144 (2006).
48. Z. Shao, H. Zhao, H. Zhao, *Nucleic Acids Res.* **37**, e16 (2009).
49. T. J. Kwiatkowski Jr., H. Y. Zoghbi, S. A. Ledbetter, K. A. Ellison, A. C. Chinault, *Nucleic Acids Res.* **18**, 7191–7192 (1990).
50. F. Sainsbury, E. C. Thuenemann, G. P. Lomonossoff, *Plant Biotechnol. J.* **7**, 682–693 (2009).
51. A. Gesell *et al*., *J. Biol. Chem.* **284**, 24432–24442 (2009).
52. A. Nakagawa *et al*., *Sci. Rep.* **4**, 6695 (2014).
53. S. Valent, M. Tóth, *Int. J. Biochem. Cell Biol.* **36**, 1266–1280 (2004).
54. L. A. Hazelwood, J. M. Daran, A. J. van Maris, J. T. Pronk, J. R. Dickinson, *Appl. Environ. Microbiol.* **74**, 2259–2266 (2008).
55. J. M. Hagel, P. J. Facchini, *Nat. Chem. Biol.* **6**, 273–275 (2010).
56. W. Li, D. T. Rossi, S. T. Fountain, *J. Pharm. Biomed. Anal.* **24**, 325–333 (2000).
57. J. Schmidt, K. Raith, C. Boettcher, M. H. Zenk, *Eur. J. Mass Spectrom.* **11**, 325–333 (2005).
58. K. Raith *et al*., *J. Am. Soc. Mass Spectrom.* **14**, 1262–1269 (2003).
59. V. V. Kushnirov, *Yeast* **16**, 857–860 (2000).
60. K. Fukuda, K. Asano, K. Ouchi, S. Takasawa, *J. Ferment. Bioeng.* **74**, 117–119 (1992).
61. T. Schmidheini, P. Sperisen, G. Paravicini, R. Hütter, G. Braus, *J. Bacteriol.* **171**, 1245–1253 (1989).
62. C. Taxis, M. Knop, *Biotechniques* **40**, 73–78 (2006).
63. U. Gueldener, J. Heinisch, G. J. Koehler, D. Voss, J. H. Hegemann, *Nucleic Acids Res.* **30**, e23 (2002).
64. S. C. Daubner *et al*., *J. Mol. Biol.* **359**, 299–307 (2006).
65. K. Hawkins, thesis, California Institute of Technology (2008).
66. R. S. Sikorski, P. Hieter, *Genetics* **122**, 19–27 (1989).


## ACKNOWLEDGMENTS

We thank Stanford Cell Sciences Imaging Facility for providing fluorescence microscopy access (Leica SP5, NIH grant SIG 1S10RR02557401) and training; Agilent Technologies for an award through their Global Academic Research Support Program; T. Kutchan and P. Facchini for contributing *Papaver* samples to the 1KP and PMS transcriptome projects, respectively; W. Lau of the Sattely laboratory for training, growing plants, and helpful discussions regarding plant experiments; and Y. Li, Y.-H. Wang, A. P. Klein, D. Endy for valuable feedback in the preparation of the manuscript. Supported by NIH grant AT007886 (C.D.S.), a NSF fellowship (S.G., I.J.T.), an ARCS Foundation fellowship (I.J.T.), a Stanford University fellowship (S.G.), and a Stanford Research Experiences for Undergraduates fellowship (M.F.I.). Strains making controlled substances (e.g., thebaine, hydrocodone) can only be provided to laboratories/institutions that have the appropriate approvals and licenses (e.g., DEA permits). Stanford University has a pending patent application on this work on which S.G., K.T., I.J.T., and C.D.S. are inventors. C.D.S., K.T., and I.J.T. are co-founders of Antheia Inc.

## SUPPLEMENTARY MATERIALS

www.sciencemag.org/content/349/6252/1095/suppl/DC1
Materials and Methods
Figs. S1 to S8
Tables S1 to S8
References (*43*–*66*)

1 July 2015; accepted 5 August 2015
Published online 13 August 2015
10.1126/science.aac9373

**Complete biosynthesis of opioids in yeast**
Stephanie Galanie *et al.*
*Science* **349**, 1095 (2015);
DOI: 10.1126/science.aac9373